

Research Article

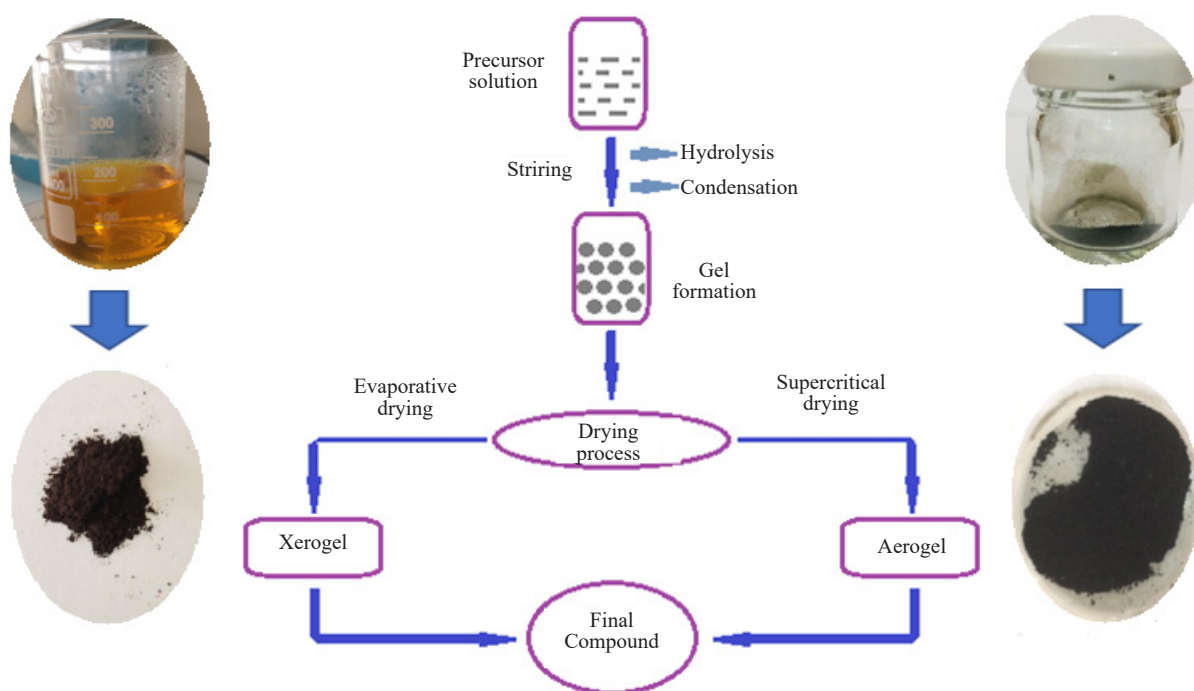
Investigation of Morphology and Structure of Cobalt Oxide (Co_3O_4) and Barium Hexaferrite ($\text{BaFe}_{12}\text{O}_{19}$) Synthesized by Sol-Gel

Mohamed Yousef Ali Issa^{ID}, Gül Yılmaz Atay^{ID*}

Department of Metallurgical and Materials Engineering, Izmir Katip Celebi University, Cigli, Izmir, Turkey
E-mail: gul.yilmaz.atay@ikc.edu.tr

Received: 5 December 2024; Revised: 25 February 2025; Accepted: 28 February 2025

Graphical Abstract:



Abstract: Sol-gel, which can generally be defined as a chemical process in which small molecules of metal alkoxides are used to produce solid materials, is an important nanomaterial synthesis method that has become very popular recently. Objects with different geometries can be coated homogeneously, and pure powders and thin films can be prepared at low temperatures, also attracting attention with its low cost compared to other production methods. In this

study, the synthesis of cobalt oxide (Co_3O_4) and barium hexaferrite ($\text{BaFe}_{12}\text{O}_{19}$), which are mostly used in the defence industry for applications such as radar absorption, shielding, stealth, and also for protecting human health from the harmful effects of radar signals, were investigated with the sol-gel method. Cobalt (II) nitrate hexahydrate and ethylene glycol were used as the precursor and solvent in cobalt oxide synthesis. In barium hexaferrite synthesis, iron (III) nitrate nonahydrate $\text{Fe}(\text{NO}_3)_3 \cdot 9\text{H}_2\text{O}$, barium nitride Ba_3N_2 , and citric acid were used as starting materials. The powders obtained at the end of the synthesis were first examined structurally by X-ray diffraction (XRD) and scanning electron microscopy-energy dispersive spectroscopy (SEM-EDS). Differential thermal analysis determined their behaviour towards heat. Particle size analysis was performed. Finally, their magnetic properties, as an important parameter used in radar absorption applications, were investigated with a vibrating sample magnetometer (VSM). Accordingly, when an external field is applied, barium hexaferrite is more magnetically soft and exhibits a strong ferromagnetism behaviour at room temperature.

Keywords: sol-gel, cobalt oxide, barium hexaferrite

1. Introduction

Sol-gel is one of the most successful chemical methods of synthesizing thin films and nanostructured materials. It has been intensively studied since the mid-1940s; however, it was not widely developed until the end of the 20th century. Usually, that process involves the transformation of the precursor solution into an inorganic solid “sol”. Various forms, for example, thin films, fibres, and powders, can be made with the sol process. The sequence and number of stages of the process and the methodology are determined by the purpose of the material being synthesized. For instance, different drying conditions make it possible to obtain both dense xerogel-based and highly porous aerogel-based materials.¹⁻⁴

The wide application of sol-gel synthesis in science and technology is due to many advantages of this method compared to the traditional way of synthesis materials. The important advantages of the sol-gel method are the high degree of homogeneity in a multicomponent system, the ability to control the particle size and pore structure, stoichiometric composition, and the possibility of obtaining non-crystalline systems.² Moreover, the sol-gel method’s most significant advantage is its mechanical properties, allowing it to obtain fibres, needles, films, and composites deposited on a substrate.³

Generally, the sol-gel method is a set of stages, including the preparation of a precursor solution, conversion into a sol, and then into a gel due to hydrolysis and condensation processes, subsequently aging, drying, and finally, the calcination of the final product. However, recently in the literature, sols have been divided into colloidal (particles form the solid dispersed phase) and polymeric (formed based on branched macromolecules).⁴ Figure 1 shows a diagram illustrating the evolution of the material structure at different steps of the sol-gel synthesis.⁵ In the first stage, the development of separate colloidal solid nuclei with a size exceeding the critical in the solution occurs. For the formation of separate solid colloidal nuclei, the solution must be a supersaturated component, i.e., its concentration exceeded the solubility limit. After forming particle nuclei in the solution, the growth occurs by dissolving smaller particles with higher surface energy. This stage determines the morphology and phase composition of the finalized products.⁶ In the sol formation, the size dissociation of particles is determined by the duration of nucleation. As a rule, the size of crystals increases with increasing reaction time and temperature. However, particle growth processes can be controlled by changing the chemical composition and pH of the solution and introducing special chemical additives.⁷

In many cases, adding several modifying components to the composition is necessary to obtain a homogeneous and stable film-forming solution.⁸ These components may have different functional purposes. Thus, the additional solvents reduce the volume concentration of particles, slowing down the aggregation processes and increasing the gel formation time. In addition, surfactants contribute to stabilizing the colloidal solution by being adsorbed on the surface of the formed nanoparticles. The step stage is the formation of the gel from a colloidal solution and is by destabilization, and usually is carried out by changing the pH of the colloidal solution. During the formation of the gel, colloidal particles join together, and the solution loses fluidity.⁹ The duration of the transformation from sol to gel is determined by the conditions of the process and can range from a few seconds to months. The third stage is the drying

gels stage to remove the liquid that fills the space between the particles. At this stage, the initially mechanically fragile raw gel undergoes enormous shrinkage and acquires a solid state.¹⁰ The drying of the gel is the most crucial stage in synthesizing monolithic materials, enormous stresses arise in the drying of monolithic gel, and cracking and destruction of monolithic samples occur. As a result of intensive research, theoretical models and practical technological methods have been created and developed to describe the evolution of a monolithic gel during drying and produce a defect-free monolithic sample.¹¹ Adding drying control chemical additives (DCCA) helps reduce the gel structure stress during drying, thereby protecting it from cracking and ensuring the integrity of products. Some organic amines and amides (formamide, dimethylformamide, and others) are often used as DCCAs.¹² During the heat treatment of the dried material, the complete thermal decomposition of DCCA and the removal of gaseous residues occurs. The final stage is the calcination of dried gel to remove the residual organic components and strengthen the material's structure. The dried gels are usually calcined with a slow increase in temperature, such as 180 °C for 15 h, 550 °C for 6 h, and 1,000 °C for 5 h, to avoid cracking of the sol-gel material. With this synthesis process, it is possible to achieve a reduction in energy consumption and a high degree of purity of products at all synthesis stages with a minimum cost and obtain a single-phase crystal structure with a high degree of perfection, strictly stoichiometric composition, and the absence of impurity phases.¹³

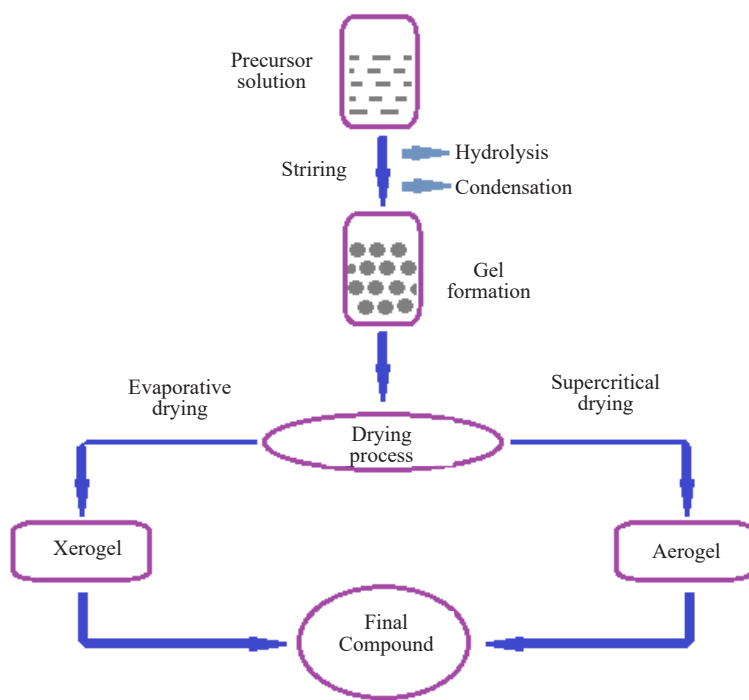


Figure 1. Sol-gel preparation steps⁷

In this study, the production of barium hexaferrite and cobalt oxide particles, which are frequently used in radio wave and microwave absorption applications, by the sol-gel method was developed, and the obtained products were examined morphologically and structurally. Barium hexaferrite is an important permanent ferrimagnetic ceramic that has attracted much attention in recent years. Its properties such as high saturation magnetization, excellent chemical stability, and high coercive force have made it used in intensive research. In addition, its high wear resistance, strong magnetocrystalline anisotropy field, high Curie temperature and good corrosion resistance make this material unique. Barium hexaferrite is usually used as electromagnetic wave absorbers and in chip inductors and microwaves. Various techniques for synthesizing barium hexaferrite have been suggested, such as the sol-gel method,¹⁴ a hydrothermal method,¹⁵ chemical precipitation,¹⁶ and the molten salt method,¹⁷ etc. All these methods involve two fundamental processes: mixing raw materials either mechanically or chemically and then heat treatment of the mixture at high

temperatures between 700 to 1,400 °C. Due to the high temperatures, the barium hexaferrite grain size in most cases is greater than 50 nm.

The chemical precipitation process and the sol-gel method of preparing have been used successively to synthesize barium hexaferrite with excellent magnetic properties, high purity, ultrafine, and good dispersion. The molten salt method has been widely used for synthesizing barium hexaferrite because it has a low synthesis temperature, and no mechanical grinding is needed. This route is based on providing a molten salt environment to react with raw material, which is much easier than a solid-state reaction. However, it has been found that the synthesis conditions of several mixed metal oxides in molten salt impact the physical properties.^{18,19} Although co-precipitation is considered one of the simplest techniques to use, the fact that ultrafine Nano-sized particles are not easy to synthesize due to particle coagulation limits the use of this technique.²⁰

Many studies have been conducted on synthesizing barium hexaferrite using sol-gel. Li et al.²¹ synthesized barium hexaferrite utilizing the sol-gel process. The raw materials were metal nitrates (iron and barium nitrates) and citric acid. First, sufficient quantities of iron nitrate and barium nitrate were dissolved in deionized water to achieve a transparent solution. Citric acid was then added to the solution and stirred for a few minutes. The solution was then heated at 60-80 °C to evaporate the water and held in a furnace at 150 °C for 48 hours. In the end, the dried gel was calcinated in the air at variable temperatures. Mozaffari et al.²² found that barium hexaferrite nanopowders can be easily obtained using goethite and barium carbonate as starting materials in the sol-gel combustion technique. Barium hexaferrite nanopowders were prepared by pouring the desired amount of goethite into distilled water. The solution was then stirred and heated. Next, citric acid, a small amount of benzoic, and acid ethylene glycol were added to the solution. Through evaporation of the water and the solution turned into an orange gel. Eventually, the burnt powders were calcinated in the air at 900 °C for 5 h to get barium hexaferrite powder. Kanagesan et al.²³ synthesized barium hexaferrite using d-fructose as a fuel. Iron (III) nitrate, nonahydrate, barium nitrate, and d-fructose were used as starting materials. First, metal nitrates and D-fructose were dissolved in deionized water, stirred continuously for 2 h to get a solution (sol), and then heated with stirring until it became a sticky liquid gel. Next, the gel was preheated in a convection oven to extract the precursor powder for 2 days. Finally, the precursor calcinated at 900 °C for 3 hours to produce hexaferrite barium material.

Cobalt oxide powder, Co_3O_4 , has various applications in various industries, including anode materials for rechargeable lithium-ion batteries, catalysts, gas sensors, and magnetic materials, including data storage devices. Cobalt oxide is an essential p-type magnetic semiconductor with a spinel crystal structure. This structure is based on a close-packed cubic lattice of oxide ions, in which Co (II) ions occupy the tetrahedral centers and Co (III) ions occupy the octahedral centers. Therefore, cobalt oxide is a p-type material. Particle size and the characteristics of Co_3O_4 are exceptionally strongly related to each other. The synthesis of Co_3O_4 can be obtained in methods such as electrochemical oxidation, chemical vapor deposition (CVD), hydrothermal, sol-gel, precipitation, and microwave treatment. It is worth mentioning that properties such as particle size, shape, and degree of crystallinity are directly related to the synthesis method. However, preparing nanocrystalline Co_3O_4 is sometimes difficult and complex, as the possibility of increasing the conductivity of Co_3O_4 can affect the structure of randomly arranged nanoparticles relative to each other.²⁴

The sol-gel process can be carried out under ideal conditions in terms of the efficacy of manipulating the product's properties, energy costs, and production process. The possibility of changing the conditions of the process (temperature, pH, the ratio of components, their concentration, aging time, etc.) allows for controlling the phase composition, size, and shape of the forming particles in a wide range. This method is quite effective for obtaining highly dispersed powders.^{24,25} In this study, barium hexaferrite ($\text{BaFe}_{12}\text{O}_{19}$) and cobalt oxide (Co_3O_4), which are used especially in radar absorbing applications, were synthesized and structurally examined and their magnetic behaviors were investigated. The obtained data were interpreted by combining with the information in the literature. After manufacturing, the powders were analyzed and characterized by using various characterization techniques such as differential thermal analysis, X-ray diffractions (XRD), vibrating sample magnetometer (VSM), and scanning electron microscopy (SEM).

2. Material and methods

Polyester resins were supplied by Verpol Boya and used as a matrix in this study to fabricate composite samples. Sigma Aldrich supplied Iron (III) nitrate nonahydrate $\text{Fe}(\text{NO}_3)_3 \cdot 9\text{H}_2\text{O}$, barium nitride Ba_3N_2 , and ethylene glycol. Cobalt (II) nitrate hexahydrate $\text{Co}(\text{NO}_3)_2 \cdot 6\text{H}_2\text{O}$ was ordered from Feta Educational Tools Center (Edulab). All chemicals have been used directly at analytical reagent grade without further purification.

Iron nitride, barium nitride and citric acid were used as starting materials in the synthesis process. Initially, a certain amount of Iron (III) nitrate nonahydrate $\text{Fe}(\text{NO}_3)_3 \cdot 9\text{H}_2\text{O}$ and barium nitride (Ba_3N_2) with a molar ratio of 12 were dissolved in deionized water at room temperature in 10 minutes. After obtaining a clear solution in this way, citric acid was added to this solution and mixed for 30 minutes. pH value was stabilized to 7 at room temperature. The mixing process was then continued on a hot plate at 80 °C to ensure evaporation. And it was dried. The solution was turned into a sticky liquid, forming a gel after evaporation of the water. Next, the gel was held in an oven at 200 °C for 12 h. Finally, the dried gel was calcined at 850 °C for 1 hour. The calcination temperature was estimated from thermogravimetric analysis (TGA)/differential scanning calorimeters (DSC) analysis of the dried gel. Figure 2 and Figure 3 demonstrate the synthetization steps of barium hexaferrite.

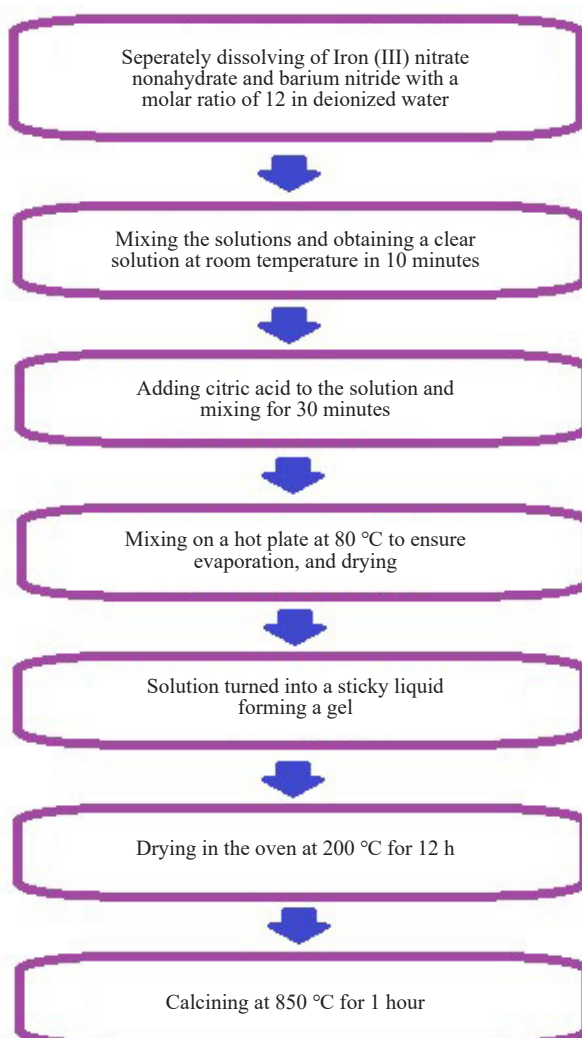


Figure 2. Synthetization steps of barium ferrite powders

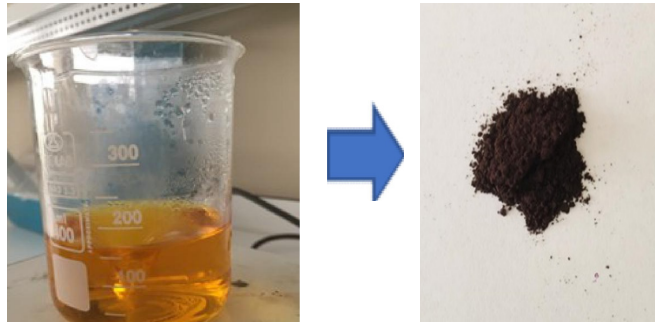


Figure 3. Synthesis steps of Barium hexaferrite powder

Cobalt (II) nitrate hexahydrate and ethylene glycol were used as precursor and solvent in the synthesis process of cobalt oxide. Cobalt (II) nitrate hexahydrate was added into ethylene solvent at a ratio of 1 : 3. Then, the solid was completely dissolved by stirring the solution at room temperature for two hours. The mixing process continued on the hot plate at 90 °C, and when the solution turned into a gel, it was evaporated to dryness. The gel was first dried by keeping it in the oven at 120 °C for 4 hours, and then calcined at 700 °C for one hour. The cobalt oxide powder obtained after calcination is shown in Figure 4 and Figure 5.

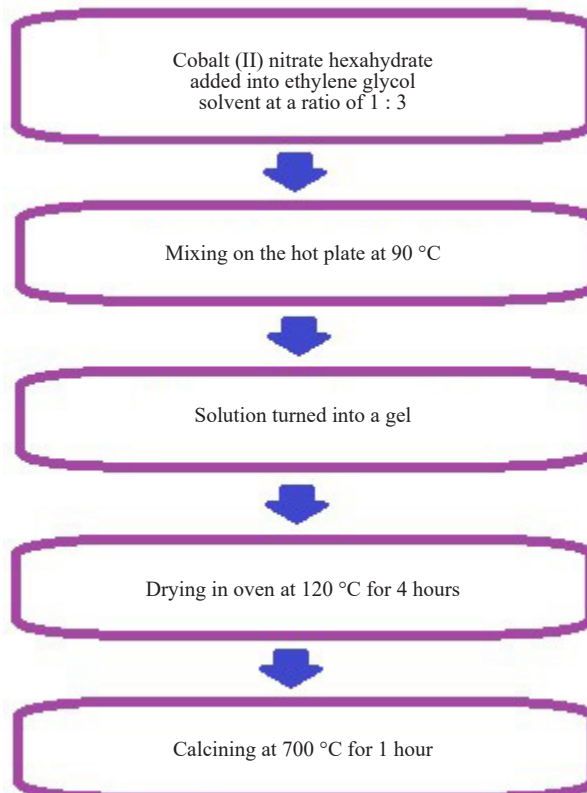


Figure 4. Synthesis steps of cobalt oxide powders

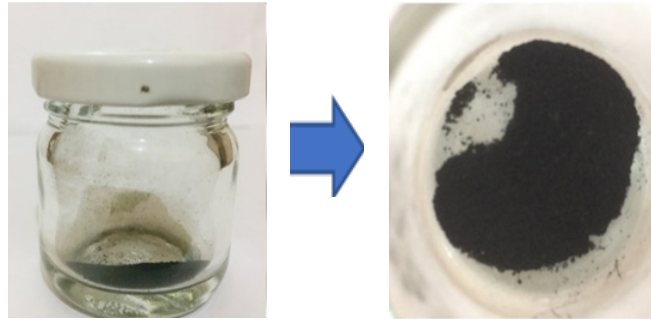


Figure 5. Synthesis steps of Cobalt oxide powder

The phase analysis of the powders was done with an Empyrean X-ray diffractometer using Cu K_α irradiation ($= 1.540 \text{ \AA}$) in the 2θ range of $20\text{-}80^\circ$. A scanning electron microscope Carl Zeiss Sigma 300 VP was used to obtain the morphological images of composites. A laser diffraction machine from Malvern Instruments, Mastersizer 2,000 was used to obtain the particle size distribution of the powders. Thermal behaviours were evaluated to observe decomposition and phase formation at a heating rate of $10 \text{ }^\circ\text{C}/\text{min}$ in a range of $25\text{-}700 \text{ }^\circ\text{C}$ under air atmosphere by using the DTA/TG machine Perkin Elmer. The magnetic properties were investigated by using a VSM 550-100 vibrating sample magnetometer.

3. Results and discussion

X-ray diffraction (XRD) was conducted to identify phases in the material (Figure 6). The XRD diffraction patterns of the synthesized $\text{BaFe}_{12}\text{O}_{19}$ powder, as shown in Figure 6a, indicate a single-phase product with only sharp diffraction peaks characteristic of crystalline material. All diffraction peaks are typical to the reference indexed as barium hexaferrite corresponding to Joint Committee on Powder Diffraction Standards (JCPDS) card no. 00-007-0276, and no impurity or other phases were detected. Therefore, this result is similar to the results reported in the previous studies.²⁶⁻²⁸ Figure 6b shows the XRD pattern of synthesized cobalt oxide Co_3O_4 . The XRD pattern is compatible with the standard spectrum of Co_3O_4 (JCPDS card no.00-042-1467), and no impurity-related peaks are detected, indicating that Co_3O_4 is the dominant compound and pure Co_3O_4 was well synthesized. Furthermore, it is similar to previous studies, which show that the low ratio in precursor and dissolvent leads to the formation of Co_3O_4 rather than CoO .^{29,30}

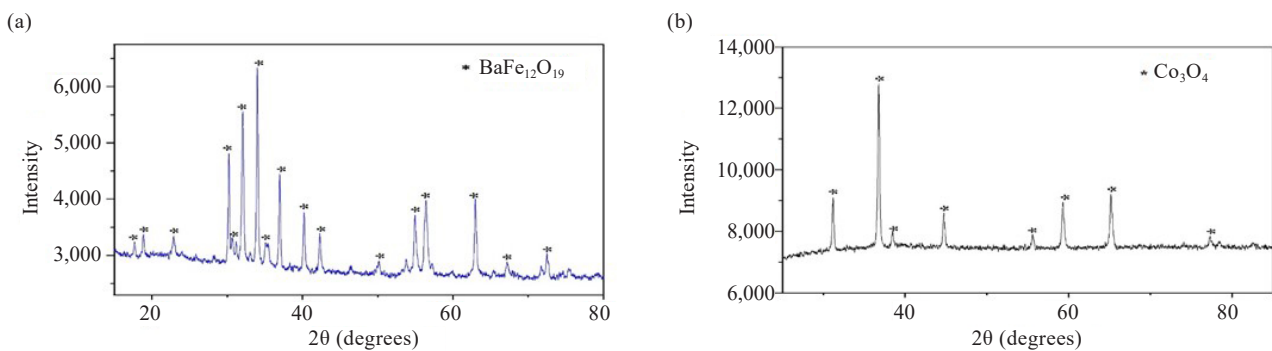


Figure 6. XRD pattern of (a) Barium hexaferrite, (b) Cobalt oxide

SEM micrographs provided reliable information about particle sizes and shapes. SEM images of the barium hexaferrite are shown in Figure 7. The micrographs were taken at magnifications of $250 \times$, 1.0 kx , and 5.0 kx . The SEM

image shows micro-size particles of barium hexaferrite of different sizes and shapes are distributed and agglomerated. According to Asiri et al.,³¹ the agglomerates are mainly due to magnetic dipole-dipole interaction between particles; moreover, a few large particles or agglomerates in a sample cannot undesirably impact the microwave absorption properties. SEM images (Figure 8) of cobalt oxide show that the powder mainly consists of different shapes of particles with microparticles. All obtained Co_3O_4 powders were hollow microspheres with a diameter of 0.5 to 10 μm . Regarding its mechanism, it can be said that nanosheets grow on the surface of the microsphere and the microspheres slowly dissolve from the inside, eventually forming hollow microspheres consisting of nanosheets.³² Generally, the synthesis method and chemical parameters significantly impact the powder's morphology. However, increasing the calcination temperature usually changes particle morphology in the sol-gel process. High temperatures can produce activation energies, increasing the growth rate and, therefore, grain size forming a bigger particle.³³ However, the morphology is quite similar to that reported by Sardjono et al.³⁴

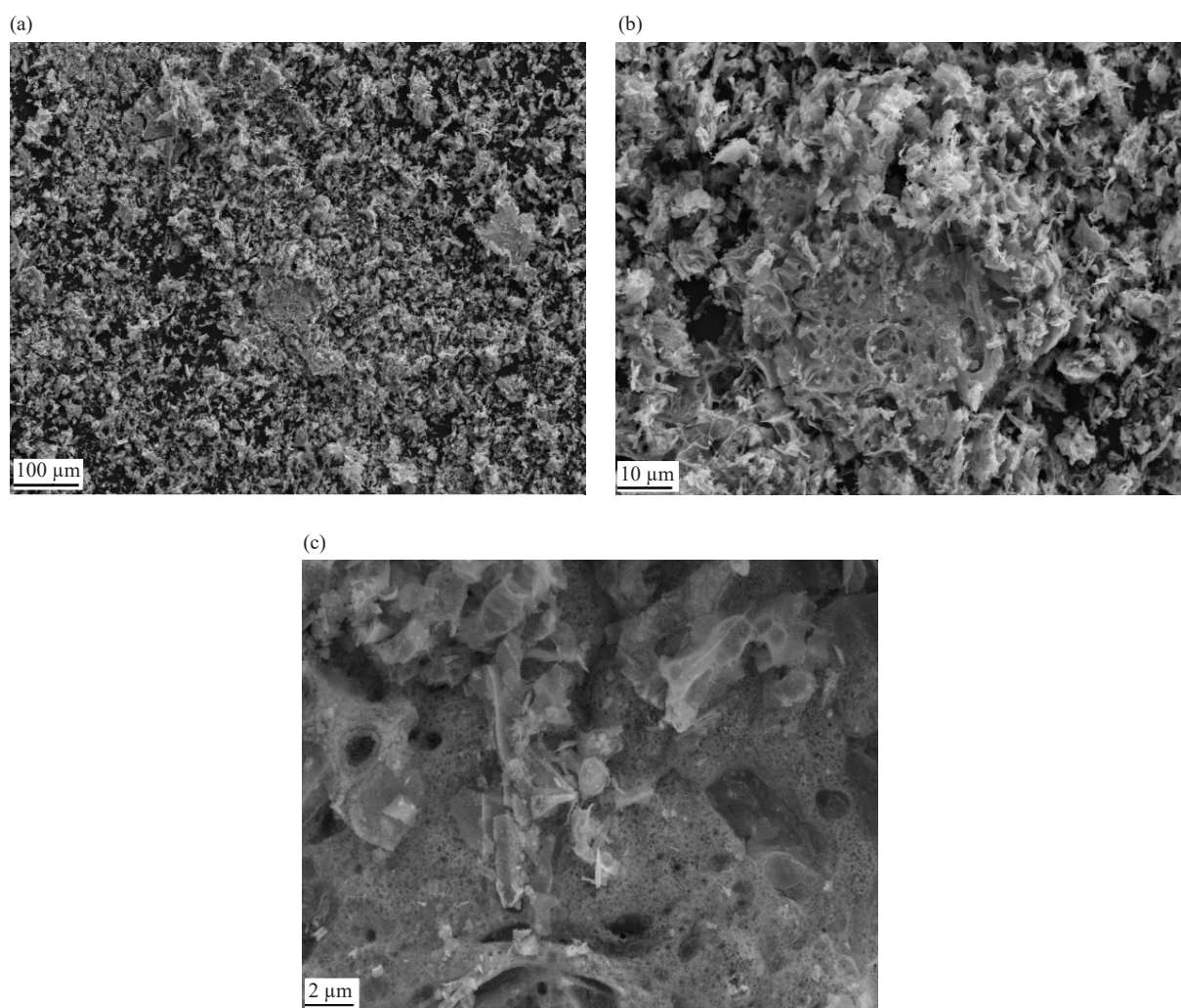


Figure 7. SEM images of Barium hexaferrite (a) 250 x (b) 1.00 kx (c) 5 kx magnifications

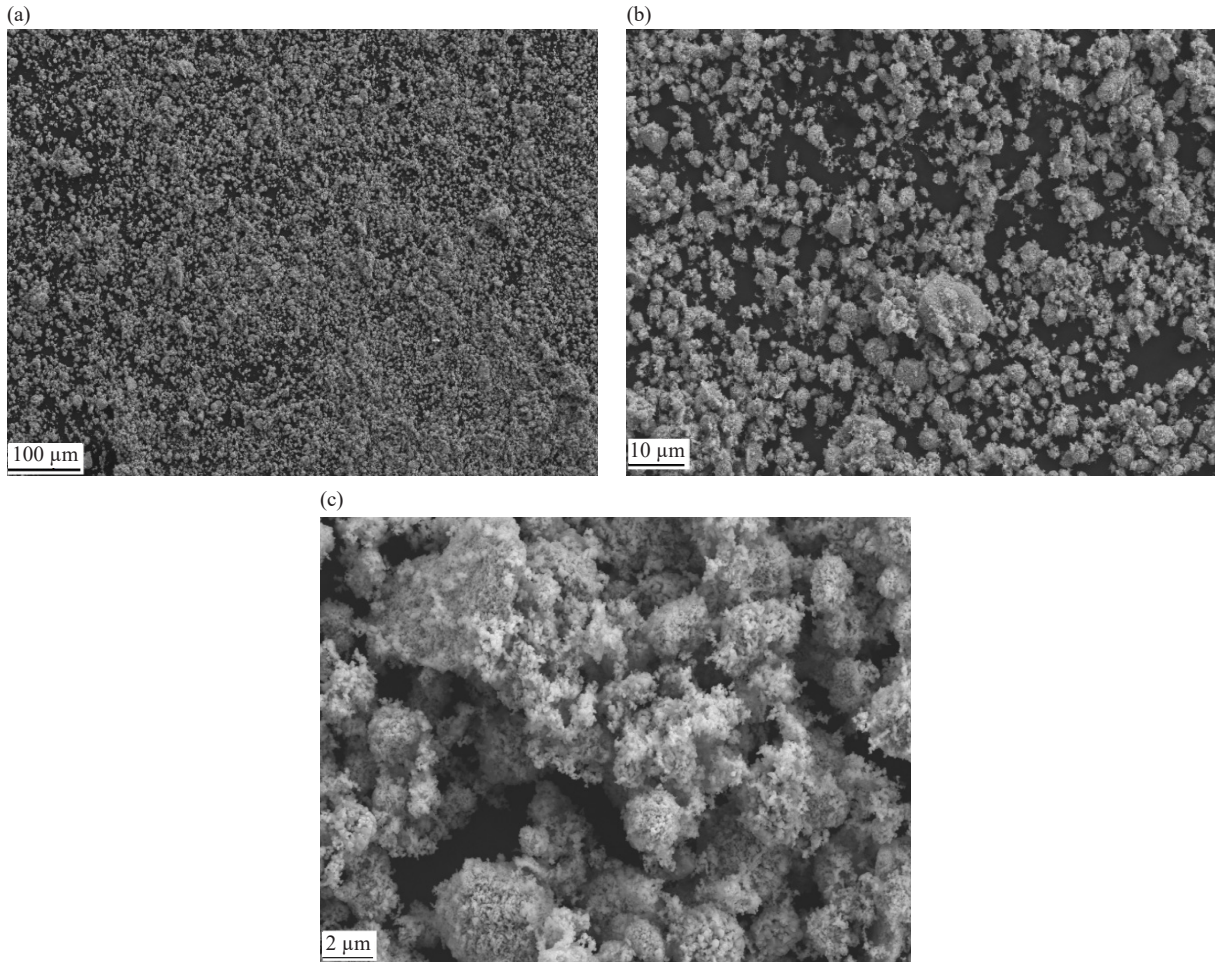


Figure 8. SEM images of Cobalt oxide (a) 250 x (b) 1.00 kx (c) 5 kx magnification

The energy dispersive X-ray (EDX) analysis was performed to analysis the elemental composition. The EDX analysis of barium hexaferrite and the relative atomic and weight abundance of Ba, Fe, O, Ti, and C are presented in Figure 9a. The EDX spectrum confirms the presence of Ba, Fe, and O. EDX analysis of cobalt oxide and the relative atomic and weight abundance of Co, O is presented in Figure 9b. The EDX spectrum shows the presence of only two elements, Co and O; no other elements were detected, confirming XRD results.

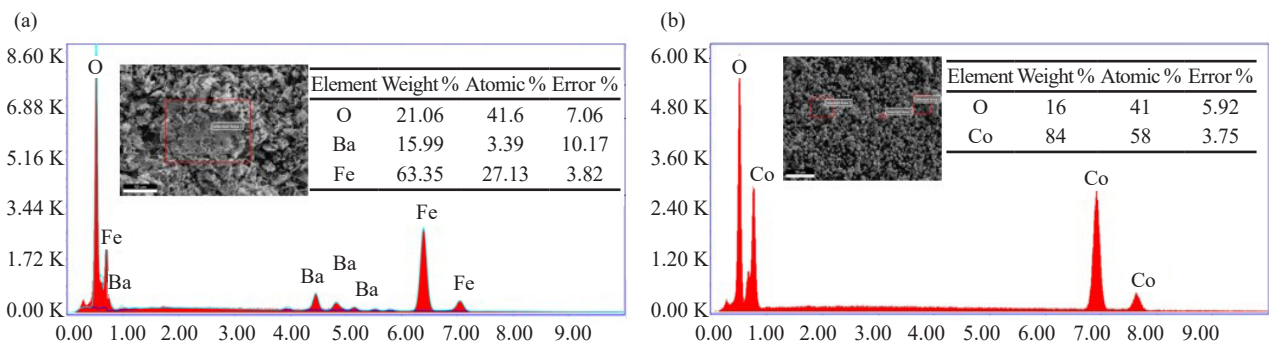


Figure 9. EDX spectrum of (a) Barium hexaferrite and (b) Cobalt oxide

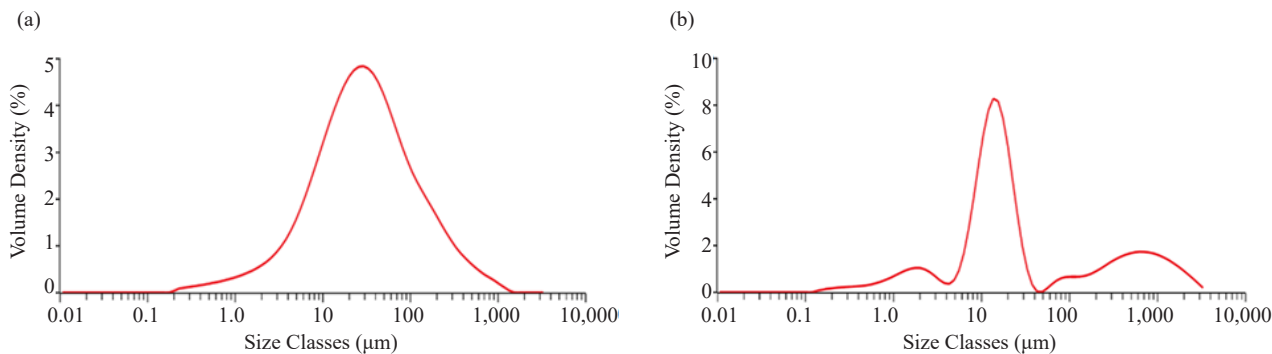


Figure 10. Particle size distribution of (a) Barium hexaferrite, and (b) Cobalt oxide

Figure 10a shows the particle distribution of barium hexaferrite. Average particle sizes of barium hexaferrite vary mainly in the range from 10 to 100 μm , the smallest fixed particles have a size of 10 μm , and the largest was about 504 μm . The average particle size is quite large compared to other works that used the same approach.^{26,35} This could be attributed to the calcination temperature as the particle size highly depends on the calcination temperature and milling time which is pointed out by Junliang et al. It is seen that materials sintered at higher sintering temperatures have larger grain sizes. On the other hand, the sintering time is as important as the sintering temperature. As sintering time increases, the density of grain boundaries decreases and subsequently, the growth of grains occurs.³⁶

Particle size distribution of cobalt oxide powder showed that 4.87% of particles have a size from 0.1 to 4 μm and 76% from 4-40 μm (Figure 10b). The large scatter is associated with the tendency for particle agglomeration during synthesis. The sol-gel method is quite effective for obtaining highly dispersed powders. However, currently, there is a lack of information in the published articles on synthesizing cobalt oxide using the sol-gel method. Therefore, the observations in this study cannot be compared to the previous studies. However, Dippong et al.³⁷ suggested that the cobalt nitrate and ethylene glycol molar ratio is more likely to impact the particle size.

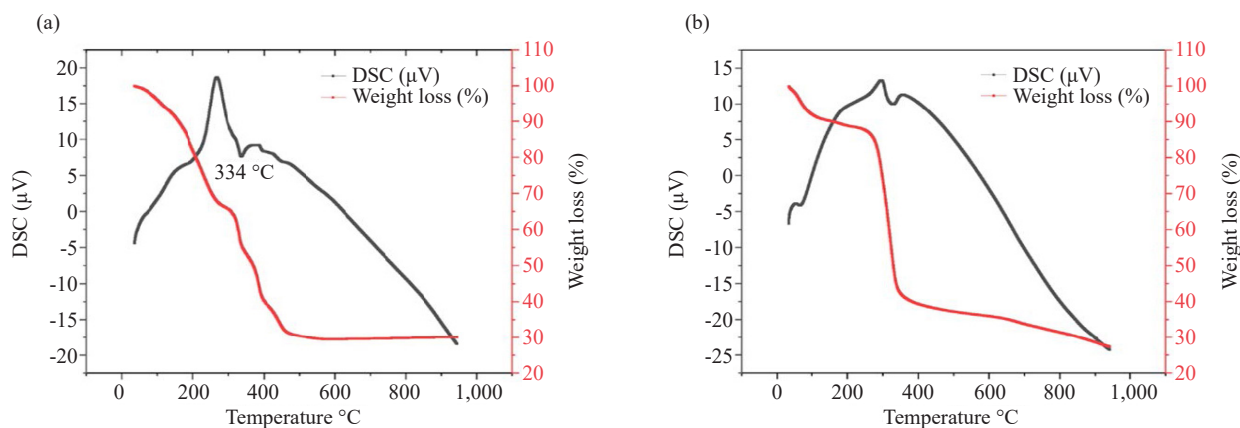


Figure 11. TGA/DSC curve of (a) Barium hexaferrite and (b) Cobalt oxide

The thermogravimetric analysis was performed to study the phase formation temperature of synthesized powders. The TGA/DSC curves for the nitrate-citrate dried gel are presented in Figure 11a. The mass loss was mainly in the temperature range of 35-495 $^{\circ}\text{C}$, which corresponds to a strong exothermic peak and endothermic on the DSC curve at 285.31 $^{\circ}\text{C}$ and 159.71 $^{\circ}\text{C}$ respectively, and this could be attributed to the reaction of nitrates with citric acid and removal of residual water-related to the decomposition reaction of the carboxyl group. A. Moreover, from 450 $^{\circ}\text{C}$ to 950 $^{\circ}\text{C}$, the weight of the dried gel was not recorded in the TGA curve and remained reasonably constant afterward, indicating

that the chemical reaction had been completed during the combustion reaction without considerable formation of other phases.³⁸ The total weight loss of the two steps is about 70.28%, similar to the observation reported by Mali and Ataie,³⁹ where a total mass loss of 70.52% was reported. The results of the X-ray phase analysis confirm the data obtained. Therefore, barium hexaferrite samples were calcined at a temperature above 500 °C.

Furthermore, the TGA/DSC curve for dried cobalt oxide gel, as presented in Figure 11b, shows that the weight loss can be differentiated into three regions. A weight loss of 11.6% was detected in the first region from 0 °C to 197.34 °C. An apparent weight loss of 49.77% in the TGA curve was observed in the second stage from 297.34 °C to 348.56 with an exothermic peak at 252.8 °C in the DSC curve, which corresponds to the decomposition reaction of the complex through an intramolecular redox process of $\text{Co}(\text{NO}_3)_2$ and $\text{C}_2\text{H}_6\text{O}_2$. Finally, a weight loss of 17.87% in the TGA curve was observed in the third stage between 348.5 °C and 960 °C, and one weak endothermic peak appeared at 397.37 °C in the DSC curve, which was due to the further combustion of the of unreacted residues. Notwithstanding, the precise reaction is unknown, and intermediates and gaseous products have not been explicitly identified, but the result agrees with previous studies data.^{40,41} The weight of the dried gel was not decreased in the TGA curve when the temperature was higher than 452 °C.

Table 1. Magnetic properties of the synthesized samples

Sample	M_s	H_c	M_r	M_r/M_s
Cobalt oxide	0.60	131.86 Oe	0.04	0.068
Barium hexaferrite	54	4,298 Oe	30.79	0.570

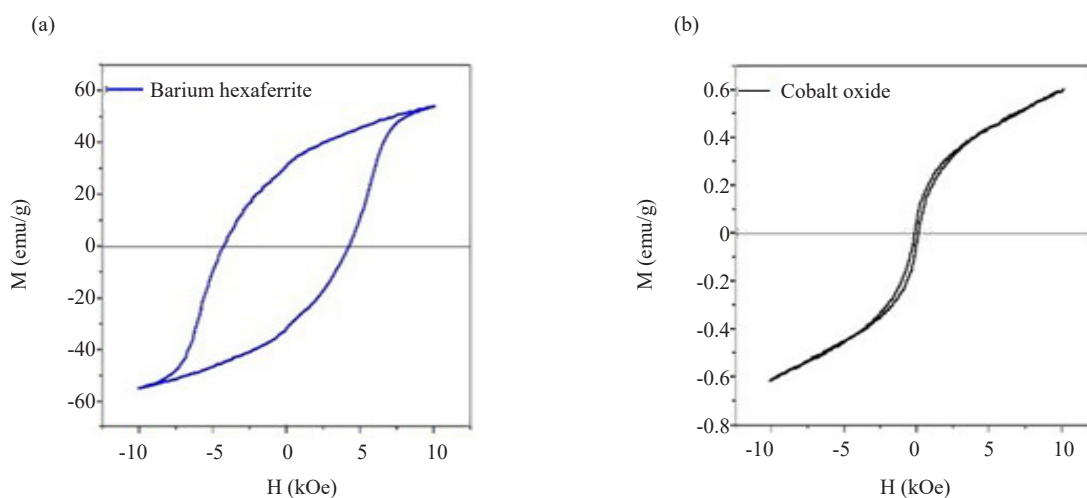


Figure 12. Magnetic hysteresis loop of (a) barium hexaferrite and (b) cobalt oxide

Room temperature hysteresis loops of barium hexaferrite and cobalt oxide are shown in Figure 12. The values of saturation magnetization (M_s), coercivity (H_c), and remnant magnetization (M_r) determined from hysteresis loops are presented in Table 1. The hysteresis loops indicated that only barium hexaferrite was magnetically soft when an external field was applied and exhibited strong ferromagnetism behaviour at room temperature. The saturation magnetization M_s value of barium hexaferrite under a field of 10 kOe was 54 emu/g. Despite the average particle size of barium hexaferrite in this work being quite large compared to the reported in the literature, the observed M_s value does not significantly differ from the reported values in the previous studies. A similar observation was made by Shepherd,⁴² which confirms that saturation magnetization is mainly unaffected by particle size. However, according to Xu et al.,⁴³

the magnetic properties of the powders are influenced significantly by calcination temperature. Due to the fact that calcination temperature has a significant effect on the morphology and phases of the synthesized powder.

Furthermore, the coercivity value 4,298 Oe was observed for barium hexaferrite, which is as much as 20% smaller than those reported values in the previous studies.⁴⁴⁻⁴⁶ This can be explained as an effect of many factors. Shalini et al.⁴⁷ argued that the composition, crystal structure, shape and size of the grains, and inter-granular interactions affect the coercivity of the powder. However, in the study conducted by Shieddieque et al., the production of barium hexaferrite from nitrate compounds by the sol-gel method for magnetic materials was investigated. In order to see the effect on the morphology, crystal structure and magnetic properties of barium hexaferrite magnets, changes in the aging time of 0 h, 2 h, 4 h and 6 h were added. Accordingly, it was observed that the synthesized particle size decreased as the aging time increased, and it was determined that different aging times did not affect the magnetic properties of barium hexaferrite.⁴⁸

On the other hand, the saturation magnetization and coercivity for cobalt oxide Co_3O_4 were found to be 0.60 emu/g and 131 Oe, respectively. The observed values of cobalt oxide are comparable to the reported values in the literature.⁴⁹⁻⁵¹ Although there has been extensive research on Co_3O_4 , studies on its critical magnetic behaviour are still controversial. However, the magnetic properties highly depend on particle size, structure, and morphology.⁵² In addition, the calcination temperature plays an important role. The saturation magnetization (M_s), and coercivity (H_c), decrease as the calcination temperature increases. In the study of Yuko and Saori, where they investigated the size-dependent magnetic properties of Co_3O_4 nanoparticles, magnetization measurements were performed on Co_3O_4 nanoparticles of various sizes. Accordingly, it was observed that saturation magnetization increased significantly at particle sizes below approximately 10 nm. It was stated that this could be due to surface rotations of small particles due to magnetic anomalies that depend on particle size.⁵³ Sardjono and Puspitasari produced cobalt oxide with sol-gel in their study where sintering time was investigated. The sintering process was carried out at 700 °C for one, two and three hours. They obtained information that the sample sintered for two hours had the smallest crystallinity and the highest peak.⁵⁴ In the study conducted by Lakra et al., cobalt oxide was synthesized by precipitation approach using cobalt nitrate. The study confirmed the crystalline nature of the particles with the size of 100 nm on average, while the SEM micrograph showed that Co_3O_4 had a sphere-like morphology.⁵⁵ In addition, in the study conducted by Li et al., they investigated the electromagnetic wave absorption properties of cobalt particles. In the study, it was revealed that the M_s of Co particles with different morphologies were similar, but the sword-like particles with larger aspect ratios on the particle surface compared to the spherical ones had higher H_c .⁵⁶

The size of the budgets allocated to defence industry projects is known. In fact, the European Commission announced 246 million US dollars for disruptive technology and European defence industry projects in 2020. Moreover, it is estimated that the radar absorber material market in this field will grow by 19% by 2027.⁵⁷ Therefore, it is obvious that demand for materials such as barium hexaferrite and cobalt oxide used in this sector will also increase. This study will guide other researchers in the production of high-performance, lightweight and at the same time economical materials.

4. Conclusions

In the study, cobalt oxide (Co_3O_4) and barium hexaferrite ($\text{BaFe}_{12}\text{O}_{19}$), which are used in many areas such as radar absorption, shielding and stealth in the defence industry and to protect against the harmful effects of radar signals, were successfully synthesized using the sol-gel method. Barium hexaferrite powder was synthesized by the sol-gel method using iron nitride, barium nitride and citric acid. Cobalt oxide powders were synthesized by the sol-gel method using cobalt (II) nitrate hexahydrate and ethylene glycol. VSM results show that barium hexaferrite and cobalt oxide samples exhibit superparamagnetic behaviour at room temperature. The XRD patterns of the synthesized samples are in high agreement with those of JCPDS cards in the literature. No secondary impurity phase was found. Particle analysis revealed that the average particle sizes of the synthesized barium hexaferrite were mainly in the range of 10 to 100 μm . Additionally, the synthesized cobalt oxide particle sizes were 4-40 μm . In future studies, various parameters, such as sintering temperatures, can be changed and their reflections in the synthesized products can be determined.

Declaration of ethical standards

I declare that the authors have followed all ethical guidelines including authorship, citation, data reporting, and publishing original research.

Credit authorship contribution statement

G.Y.A. and M.Y.A.I. wrote the main manuscript text, prepared figures and tables, and reviewed the manuscript.

Funding/Acknowledgements

This work was supported by the İzmir Katip Çelebi University Research Funds, Grant No: 2020-TDR-FEBE-0003.

Data availability

The research data associated with this paper is presented in the paper.

Conflict of interests

I declare that the authors have no competing interests, or other interests that might be perceived to influence the results and/or discussion reported in this paper.

References

- [1] Livage, J. Basic principles of sol-gel chemistry. In *Sol-Gel Technologies for Glass Producers and Users*. Springer: Boston, MA, 2004; pp 3-14.
- [2] Bokov, D.; Turki Jalil, A.; Chupradit, S.; Suksatan W.; Javed, A. M.; Shewael, I. H.; Valiev, G. H.; Kianfar, E. Nanomaterial by sol-gel method: Synthesis and application. *Adv. Mater. Sci. Eng.* **2021**, *2021*, 5102014.
- [3] Scherer, G. W. Aging and drying of gels. *J. Non-Cryst. Solids* **1988**, *100*, 77-92.
- [4] Yoldas, B. E. Monolithic glass formation by chemical polymerization. *J. Mater. Sci.* **1979**, *14*, 1843-1849.
- [5] Nisticò, R.; Scalarone, D.; Magnacca, G. Sol-gel chemistry, templating and spin-coating deposition: A combined approach to control in a simple way the porosity of inorganic thin films/coatings. *Microporous Mesoporous Mater.* **2017**, *248*, 18-29.
- [6] Catauro, M.; Tranquillo, E.; Dal, P. G.; Pasquali, M.; Dell'Era, A.; Vecchio, C. S. Influence of the heat treatment on the particles size and on the crystalline phase of TiO₂ synthesized by the sol-gel method. *Materials* **2018**, *11*, 2312-2364.
- [7] Lakshmi, B. B.; Patrissi, C. J.; Martin, C. R. Sol-gel template synthesis of semiconductor oxide micro- and nanostructures. *Chem. Mater.* **1997**, *9*, 2544-2550.
- [8] Yilmaz, E.; Soylak, M. Functionalized nanomaterials for sample preparation methods. In *Handbook of Nanomaterials in Analytical Chemistry*, Elsevier: Amsterdam, 2020; pp 375-413.
- [9] Mackenzie, J. D. Applications of the sol-gel process. *J. Non-Cryst. Solids* **1988**, *100*, 162-168.
- [10] Dehghanhadikolaei, A.; Ansary, J.; Ghoreishi, R. Sol-gel process applications: A mini-review. *Proc. Nat. Res. Soc.* **2018**, *2*, 2008-2029.
- [11] Attia, Y. A. *Sol-Gel Processing and Applications*; Springer Science & Business Media: New York, 2012.
- [12] Singh, L. P.; Bhattacharyya, S. K.; Kumar, R.; Mishra, G.; Sharma, U.; Singh, G.; Ahalawat, S. Sol-gel processing of silica nanoparticles and their applications. *Adv. Colloid Interface Sci.* **2014**, *214*, 17-37.
- [13] Opuchovic, O.; Kreiza, G.; Senvaitiene, J.; Kazlauskas, K.; Beganskiene, A.; Kareiva, A. Sol-gel synthesis, characterization and application of selected sub-microsized lanthanide (Ce, Pr, Nd, Tb) ferrites. *Dyes Pigm.* **2015**,

118, 176-182.

- [14] Atay, H. Y.; Çelik, E. Barium hexaferrite reinforced polymeric dye composite coatings for radar absorbing applications. *Polym. Compos.* **2014**, *35*, 602-610.
- [15] Chen, M.; Fan, R.; Liu, G. F.; Wang, X. A.; Sun, K. Magnetic properties of barium ferrite prepared by hydrothermal synthesis. *Key Eng. Mater.* **2015**, *655*, 178-181.
- [16] Radwan, M.; Rashad, M. M.; Hessien, M. M. Synthesis and characterization of barium hexaferrite nanoparticles. *J. Mater. Process. Technol.* **2007**, *181*, 106-109.
- [17] Arendt, R. H. The molten salt synthesis of single magnetic domain BaFe₁₂O₁₉ and SrFe₁₂O₁₉ crystals. *J. Solid State Chem.* **1973**, *8*, 339-347.
- [18] Yoon, K. H.; Lee, D. H.; Jung, H. J. Molten salt synthesis of anisotropic BaFe₁₂O₁₉ powders. *J. Mater. Sci.* **1992**, *27*, 2941-2945.
- [19] Hai-Feng, L.; Rong-Zhou, G.; Xiu-Fang, L.; Wei, Y.; Xian, W.; Li-Ren, F.; Gang, H. Molten salt synthesis and magnetic properties of BaFe₁₂O₁₉ hexaferrite. *J. Inorg. Mater.* **2011**, *26*, 792-796.
- [20] Chen, D. H.; Chen, Y. Y. Synthesis of barium ferrite ultrafine particles by coprecipitation in the presence of polyacrylic acid. *J. Colloid Interface Sci.* **2001**, *235*, 9-14.
- [21] Li, Y.; Wang, Q.; Yang, H. Synthesis, characterization and magnetic properties on nanocrystalline BaFe₁₂O₁₉ ferrite. *Curr. Appl. Phys.* **2009**, *9*, 1375-1380.
- [22] Mozaffari, M.; Taheri, M.; Amighian, J. Preparation of barium hexaferrite nanopowders by the sol-gel method, using goethite. *J. Magn. Magn. Mater.* **2009**, *321*, 1285-1289.
- [23] Kanagesan, S.; Juesurani, S.; Velmurugan, R.; Kumar, C. Synthesis of barium hexaferrite (BaFe₁₂O₁₉) using D-fructose as fuel. *J. Manuf. Eng.* **2010**, *5*, 133-136.
- [24] Janjua, M. R. S. A. Synthesis of Co₃O₄ nano aggregates by co-precipitation method and its catalytic and fuel additive applications. *Open Chem.* **2019**, *17*, 865-873.
- [25] Dippong, T.; Goga, F.; Avram, A. Influence of the cobalt nitrate: Ethylene glycol molar ratio on the formation of carboxylate precursors and cobalt oxides. *Stud. Univ. Babeş-Bolyai Chem.* **2017**, *62*, 165-177.
- [26] Junliang, L.; Yanwei, Z.; Cuijing, G.; Wei, Z.; Xiaowei, Y. One-step synthesis of barium hexaferrite nano-powders via microwave-assisted sol-gel auto-combustion. *J. Eur. Ceram. Soc.* **2010**, *30*, 993-997.
- [27] Meng, Y. Y.; He, M. H.; Zeng, Q.; Jiao, D. L.; Shukla, S.; Ramanujan, R. V.; Liu, Z. W. Synthesis of barium ferrite ultrafine powders by a sol-gel combustion method using glycine gels. *J. Alloys Compd.* **2014**, *583*, 220-225.
- [28] Surig, C.; Hempel, K. A.; Bonnenberg, D. Hexaferrite particles prepared by sol-gel technique. *IEEE Trans. Magn.* **1994**, *30*, 4092-4094.
- [29] Armelao, L.; Barreca, D.; Gross, S.; Martucci, A.; Tieto, M.; Tondello, E. Cobalt oxide-based films: Sol-gel synthesis and characterization. *J. Non-Cryst. Solids* **2001**, *293*, 477-482.
- [30] Barrera, E.; Viveros, T.; Avila, A.; Quintana, P.; Morales, M.; Batina, N. Cobalt oxide films grown by a dipping sol-gel process. *Thin Solid Films* **1999**, *346*, 138-144.
- [31] Asiri, S.; Güner, S.; Demir, A. Y.; Yildiz, A.; Manikandan, A.; Baykal, A. Synthesis and magnetic characterization of Cu substituted barium hexaferrites. *J. Inorg. Organomet. Polym.* **2018**, *28*, 1065-1071.
- [32] Tao, F.; Gao, C.; Wen, Z.; Wang, Q.; Li, J.; Xu, Z. Cobalt oxide hollow microspheres with micro- and nano-scale composite structure: Fabrication and electrochemical performance. *J. Solid State Chem.* **2009**, *182*, 1055-1060.
- [33] Irvani, S.; Varma, R. S. Sustainable synthesis of cobalt and cobalt oxide nanoparticles and their catalytic and biomedical applications. *Green Chem.* **2020**, *22*, 2643-2661.
- [34] Sardjono, S. A.; Puspitasari, P. Synthesis and characterization of cobalt oxide nanoparticles using sol-gel method. *AIP Conf. Proc.* **2020**, *2231*, 040046.
- [35] Mohebbi, E.; Hasani, S.; Nouri-Khezrabad, M.; Ziarati, A. The effect of agarose agent on the structural, magnetic and optical properties of barium hexaferrite nano-particles synthesized by sol-gel auto-combustion method. *Ceram. Int.* **2023**, *49*, 9757-9770.
- [36] Junliang, L.; Wei, Z.; Cuijing, G.; Yanwei, Z. Synthesis and magnetic properties of quasi-single domain M-type barium hexaferrite powders via sol-gel auto-combustion: Effects of pH and the ratio of citric acid to metal ions (CA/M). *J. Alloys Compd.* **2009**, *479*, 863-869.
- [37] Dippong, T.; Goga, F.; Avram, A. Influence of the cobalt nitrate: Ethylene glycol molar ratio on the formation of carboxylate precursors and cobalt oxides. *Studia UBB. Chemia.* **2017**, *62*, 165-176.
- [38] Yue, Z.; Zhou, J.; Li, L.; Zhang, H.; Gui, Z. Synthesis of nanocrystalline NiCuZn ferrite powders by sol-gel auto-combustion method. *J. Magn. Magn. Mater.* **2000**, *208*, 55-60.
- [39] Mali, A.; Ataie, A. Structural characterization of nano-crystalline BaFe₁₂O₁₉ powders synthesized by sol-gel

- combustion route. *Scr. Mater.* **2005**, *53*, 1065-1070.
- [40] Basolo, F.; Murmann, R. K.; Whitney, J. E.; Rollinson, C. L. Acidopentamminecobalt (III) salts. *Inorg. Synth.* **1953**, *4*, 171-176.
- [41] Wendlandt, W. W. Thermal decomposition of metal complexes-III: Stoichiometry of the thermal dissociation of some hexamminecobalt (III) complexes. *J. Inorg. Nucl. Chem.* **1963**, *25*, 545-551.
- [42] Shepherd, P.; Mallick, K. K.; Green, R. J. Magnetic and structural properties of M-type barium hexaferrite prepared by co-precipitation. *J. Magn. Magn. Mater.* **2007**, *311*, 683-692.
- [43] Xu, G.; Ma, H.; Zhong, M.; Zhou, J.; Yue, Y.; He, Z. Influence of pH on characteristics of BaFe₁₂O₁₉ powder prepared by sol-gel auto-combustion. *J. Magn. Magn. Mater.* **2006**, *301*, 383-388.
- [44] Li, Y.; Wang, Q.; Yang, H. Synthesis, characterization and magnetic properties on nanocrystalline BaFe₁₂O₁₉ ferrite. *Curr. Appl. Phys.* **2009**, *9*, 1375-1380.
- [45] Yu, H. F. BaFe₁₂O₁₉ powder with high magnetization prepared by acetone-aided coprecipitation. *J. Magn. Magn. Mater.* **2013**, *341*, 79-85.
- [46] Zhong, W.; Ding, W.; Zhang, N.; Hong, J.; Yan, Q.; Du, Y. Key step in synthesis of ultrafine BaFe₁₂O₁₉ by sol-gel technique. *J. Magn. Magn. Mater.* **1997**, *168*, 196-202.
- [47] Shalini, M. G.; Subha, A.; Sahu, B.; Sahoo, S. C. Phase evolution and temperature dependent magnetic properties of nanocrystalline barium hexaferrite. *J. Mater. Sci. Mater. Electron.* **2019**, *30*, 13647-13654.
- [48] Shieddieque, A. D.; Viradhian, S.; Muttahar, M. I. Z. Characterization of barium hexaferrite (BaFe₁₂O₁₉) from nitrate compound with sol-gel method for barium hexaferrite magnetic materials. *Solid State Phenom.* **2023**, *345*, 77-84.
- [49] Ullah, A. A.; Amin, F. B.; Hossain, A. Tailoring surface morphology and magnetic property by precipitants concentrations dependent synthesis of Co₃O₄ nanoparticles. *Ceram. Int.* **2020**, *46*, 27892-27896.
- [50] Zdorovets, M. V.; Shumskaya, A. E.; Kozlovskiy, A. L. Investigation of the effect of phase transformations on the magnetic and electrical properties of Co/Co₃O₄ nanowires. *J. Magn. Magn. Mater.* **2020**, *497*, 166079.
- [51] Anandhababu, G.; Ravi, G. Facile synthesis of quantum sized Co₃O₄ nanostructures and their magnetic properties. *Nano-Struct. Nano-Objects* **2018**, *15*, 1-9.
- [52] Mammadyarova, S. J. Synthesis and characterization of cobalt oxide nanostructures: A brief review. *Azerb. Chem. J.* **2021**, *2*, 80-93.
- [53] Ichianagi, Y.; Yamada, S. The size-dependent magnetic properties of Co₃O₄ nanoparticles. *Polyhedron* **2005**, *24*, 2813-2816.
- [54] Sardjono, S. A.; Puspitasari, P. Synthesis and characterization of cobalt oxide nanoparticles using sol-gel method. *AIP Conf. Proc.* **2020**, *2231*, 040046.
- [55] Lakra, R.; Kumar, R.; Thatoi, D. N.; Sahoo, P. K.; Soam, A. Synthesis and characterization of cobalt oxide (Co₃O₄) nanoparticles. *Mater. Today Proc.* **2021**, *41*, 269-271.
- [56] Li, H.; Li, H.; Sheng, B.; Zheng, B.; Shi, S.; Cai, Q.; Xu, W.; Zhao, X.; Liu, Y. Synthesis of cobalt particles and investigation of their electromagnetic wave absorption characteristics. *Materials*. **2024**, *17*, 200.
- [57] MarkNtel Advisor. *Global Radar Absorbent Material Market Research Report: Forecast (2022-2027)*. <https://www.marknteladvisors.com/research-library/global-radar-absorbent-material-market.html> (accessed May 5, 2024).